

## UC Irvine

### UC Irvine Previously Published Works

**Title**

Fluctuation Spectroscopy Analysis of Glucose Capped Gold Nanoparticles.

**Permalink**

<https://escholarship.org/uc/item/1sf6k4fb>

**Journal**

Langmuir : the ACS journal of surfaces and colloids, 32(50)

**ISSN**

0743-7463

**Authors**

Porcaro, F  
Miao, Y  
Kota, R  
et al.

**Publication Date**

2016-12-01

**DOI**

10.1021/acs.langmuir.6b02545

Peer reviewed



# HHS Public Access

Author manuscript

Langmuir. Author manuscript; available in PMC 2017 June 14.

Published in final edited form as:

Langmuir. 2016 December 20; 32(50): 13409–13417. doi:10.1021/acs.langmuir.6b02545.

## Fluctuation Spectroscopy Analysis of Glucose capped Gold Nanoparticles

F. Porcaro<sup>a,\*</sup>, Y. Miao<sup>b</sup>, R. Kota<sup>b</sup>, J. Haun<sup>b</sup>, G. Polzonetti<sup>a</sup>, C Battocchio<sup>a</sup>, and E. Gratton<sup>c,\*\*</sup>

<sup>a</sup>Roma Tre University, Dept. of Sciences, Via della Vasca Navale 79, 00146 - Rome (Italy)

<sup>b</sup>Haun Laboratory for Nanoengineering and Molecular Medicine, Biomedical Engineering Department, University of California, Irvine, USA

<sup>c</sup>Laboratory for Fluorescence Dynamics, Biomedical Engineering Department, University of California, Irvine, USA

### Abstract

In this work, we report the synthesis and biophysical studies carried out on a new kind of biocompatible and very stable gold nanoparticles (GNPs) stabilized with Glucose through a PEG linker (AuNP-PEG-Glu). The synthetic path was optimized to obtain nanoparticles of controlled sizes. Z-Potential and Dynamic Light Scattering measurements allowed assessing the nanodimension, dispersity, surface charge and stability of our GNPs. Confocal Microscopy demonstrated qualitatively that Glucose molecules are successfully bonded to GNPs surface. For our study, we selected nanoparticles with diameter in a range that maximizes the internalization efficiency in cells (40 nm). A detailed investigation about the biophysical proprieties of AuNP-PEG-Glu was carried out by means of Fluorescence Correlation Spectroscopy (FCS) and Orbital Tracking techniques. This work gives new insights about the uptake mechanism of Gold nanoparticles capped with glucose molecules.

### Keywords

Synthesis; Gold Nanoparticle; Pair Correlation; Particle Tracking

## 1. Introduction

Metal nanoparticles stabilized with specific organic ligands, *i.e.* thiols and capping molecules, are suitable to obtain, among the others, functionalized gold nanoparticles (GNPs) with good level of control on the NPs size, dispersity and shape [1]. The capping molecules give different characteristics and properties to the GNPs and their selection allows

\*Corresponding Author: francesco.porcaro@uniroma3.it telephone 57333390; fax number: 0039-06-57333390. \*\* email egratton@uci.edu telephone number: 001-949-824-2674; fax number: 001-949-824-1727.

**Author Contributions:** The manuscript was written through contributions of all authors. All authors have given approval to the final version of the manuscript.

**Supporting Information.** Figure 1S: citrate nanoparticles UV–Vis spectrum normalized in the region 450–700 nm; Figure 2S: NMR Spectrum of NHS ester of lipoic acid (LA-NHS). Figure 3S: Rough ESI-MS spectrum of NHS ester of lipoic acid (LA-NHS); Figure 4S: IR-spectra of synthetic polymer at different synthetic steps. Figure 5S. Rough ESI-MS spectrum of LA-PEG1500-NH2 and the NH2-PEG1500-NH2. This material is available free of charge via the Internet at <http://pubs.acs.org>.

tailoring for specific applications. For example, the use of gold nanoparticles in biotechnology and medicine is becoming a field of interest worldwide due to the versatility and biocompatibility of these nanostructured materials [2,3].

Many reports have recently considered synthetic procedures and characterization of GNPs obtained with different capping agents, shapes and properties [4,5,6,7]. However, the delivery of a cargo to specific cells or tissue is still a challenging question in biomedical research that is facing the problem of possible toxicity of GNPs [8,9]. Due to this concern, the use of a transfer structure, which can bind to a specific marker for tumour cells only, is a new goal of the research in biomedicine. In this context, glucose functionalization of gold nanoparticles was investigated firstly by Kong et al. [10] and Zhang and his group [11]. The glucose backbone has the characteristic of biological enhancement of uptake in vitro and can be further modified with the insertion of fluorine atom, suggesting a promising perspective to realize theragnostic devices in cancer treatment [12, 13]. In particular, glucose functionalized GNPs are believed to cross the blood brain barrier [14].

Our work aims to explore new cheaper and simpler synthetic approaches and advanced characterization of GNPs. GNPs interaction with living cells is mainly related to physical and chemical properties of the molecules used as capping agents during the synthesis process and linked to nanoparticles surface [15]. While most of the works reported in the literature focus on the uptake fate of nanoparticles functionalized by a large antibody or very small molecules as citrate, there is no general agreement in how a carbohydrate like glucose mediates the uptake of nanostructures inside the cells. However, despite the lack of a generally recognized mechanism, there is a growing interest in the study of glucose functionalized gold nanoparticles due to recent applications in brain drug delivery [14,16].

Fluorescence Correlation Spectroscopy (FCS) has emerged as a very powerful method for studying the motions of proteins in both the interior and exterior of a cell. FCS provides information at the single-molecule level by averaging the behavior of many molecules, and thus yields very good statistics. In this work we use the spatial Pair Cross-correlation Function (PCF) to measure the time a particle takes to move from one location to another by correlating the intensity fluctuations at specific points on a grid, independently of how many particles are in the imaging field. Therefore, the average path of the particles can be traced. This method can be used to detect when an object like a protein or a nanoparticle passes through the membrane barrier together with the location of the crossing site. This information cannot be obtained with the fluorescence recovery after photobleaching technique or other image current correlation spectroscopy method [17]. As a result, FCS was successfully applied in order to provide an extensive description of the NPs-Glucose-Transporter complex organization and its cell membrane localization. Indeed, other important physical parameters such as diffusion coefficient and number of receptors per particles can also be determined. However, in order to reach a full biophysical description of NPs-Transporter complex behavior inside the cell, the assessment of spatial trajectories of the complex is mandatory. In this context, another important spectroscopic tool such as Orbital Tracking techniques was exploited to complete the investigation [18].

As already described by Lanzaò and Gratton [18], Orbital Tracking is a super-resolution imaging technique able to provide the position of fluorescent molecules with nanometer precision. In FCS the molecules are observed one at the time through the use of small detection volumes at fixed locations and the molecular parameters are generally obtained by averaging many single molecule fluctuation events. In Orbital Tracking the same molecule or particle is observed for a longer period of time with respect to FCS, so that heterogeneities in time or space and subpopulations become more evident [18].

Consequently, in order to fully understand the effect of different NPs surface capping molecules on the uptake process *in vitro*, PCF and Particle Tracking seem to be the optimal techniques to elucidate the GNPs uptake mechanism. Position and direction of newly synthesized Au-PEG-Glu nanoparticles inside and outside the cells was determined by means of light-scattering signal, generated by gold high reflectance properties. With the aim of performing fluctuation experiments, HeLa cells were transfected with a glucose transporter (GLUT1) fused with Green Fluorescence Protein (GFP) and the fluorescence signal was monitored. For this work a two-photon microscope system equipped with 80 MHz Ti:Sapphire laser at 800 nm wavelength was used in order to reduce photo-bleaching of fluorescence molecules. Au-PEG-Glu scattering and fluorescence signals from GLUT1-GFP-fused protein were analyzed using the SIMFCS software available at [www.lfd.uci.edu](http://www.lfd.uci.edu).

## 2. Experimental Section

### 2.1. Chemicals and materials

All chemicals were purchased by Sigma Aldrich Co. Hydrogen tetrachloroaurate (III) trihydrate ( $\text{HAuCl}_4 \cdot 3\text{H}_2\text{O}$ , 99.9+%), sodium citrate ( $\text{Na}_3\text{C}_6\text{H}_5\text{O}_7$ ), poly(ethylene glycol) bis(amine) (PEG1500-bisamine) ( $\text{H}_2\text{N}(\text{CH}_2\text{CH}_2\text{O})_n\text{CH}_2\text{CH}_2\text{NH}_2$ ), *N*-Hydroxysuccinimide (NHS) ( $\text{C}_4\text{H}_5\text{NO}_3$ ), D-glucuronic acid ( $\text{C}_6\text{H}_{10}\text{O}_7$ ), ( $\pm$ )- $\alpha$ -lipoic acid (LA) ( $\text{C}_8\text{H}_{14}\text{O}_2\text{S}_2$ ), *N,N'*-Dicyclohexylcarbodiimide (DCC) ( $\text{C}_{13}\text{H}_{22}\text{N}_2$ ), *N*-(3-Dimethylaminopropyl)-*N'*-ethylcarbodiimide hydrochloride (EDC)  $\text{C}_8\text{H}_{17}\text{N}_3 \text{HCl}$ . Deionized water was obtained from Zeener Power I Scholar-UV (electrical resistivity 18.2 M $\Omega$ ).

### 2.2. Synthesis of Glucose functionalized Gold Nanoparticles (Au-PEG-Glu)

The synthesis of the GNPs consists in different steps and can be summed up as follows. First, according to literature reports [19], gold nanocores were produced through reduction in aqueous phase of  $\text{HAuCl}_4 \cdot 3\text{H}_2\text{O}$  with sodium citrate controlling the temperature (90° C) and varying the pH from 7 to 5. Then, a PEG polymer was properly derivatized by means of NHS chemistry [20] to bind it to the gold cores. The last step is the glucose functionalization of the Au-PEG-NH<sub>2</sub> by means of *in situ* coupling reaction. The following points describe in detail the whole synthesis.

#### 2.2.1 Synthesis of citrate capped Gold core by means of Seed-Growth method

—Gold nanocores were synthesized according to Bastus and collaborators [19] in order to fine tuning NPs diameters. Briefly, a solution of 2.2mM sodium citrate in Milli-Q water (150 mL) was heated with a heating mantle in a 250 mL three-necked round-bottomed flask for 15 min under vigorous stirring. A condenser was utilized to prevent the evaporation of the

solvent. After boiling, 1 mL of  $\text{HAuCl}_4$  (25 mM) was injected. The color of the solution changed from yellow to bluish gray and then to soft pink in 10 min; the reaction was then cooled until the temperature of the solution reached 90 °C. Then, 1 mL of sodium citrate (60 mM) and 1 mL of a  $\text{HAuCl}_4$  solution (25 mM) were sequentially injected (time delay ~2 min). After 30 min the reaction was finished. This process was repeated twice. After that, the sample was diluted by extracting 55 ml of sample and adding 53 ml of Milli-Q water and 2 ml of sodium citrate 60 mM. This solution was then used as seed solution and the process was repeated again. By repeating this process (sequential addition of sodium citrate and  $\text{HAuCl}_4$ , and extraction), up to 5 generations of citrate capped gold nanocores, named G0-G5, of progressively larger sizes were grown in the range 10-35 nm. For our purposes, we selected the fifth generation with a size of 35 nm. Main characterizations of the products are herein reported. The gold salt precursor reduction was considered 100% completed for each growth step according to the literature [19]

G0 (UV-vis,  $\lambda_{\text{max}}$  [nm],  $\text{H}_2\text{O}$ ): 517; DLS ( $\langle 2\text{RH} \rangle$  [nm],  $\text{H}_2\text{O}$ ):  $10 \pm 2$ . G1 (UV-vis,  $\lambda_{\text{max}}$  [nm],  $\text{H}_2\text{O}$ ): 519, DLS ( $\langle 2\text{RH} \rangle$  [nm],  $\text{H}_2\text{O}$ ):  $15 \pm 2$ . G2 (UV-vis,  $\lambda_{\text{max}}$  [nm],  $\text{H}_2\text{O}$ ): 520; DLS ( $\langle 2\text{RH} \rangle$  [nm],  $\text{H}_2\text{O}$ ):  $20 \pm 2$ . G3 (UV-vis,  $\lambda_{\text{max}}$  [nm],  $\text{H}_2\text{O}$ ): 521; DLS ( $\langle 2\text{RH} \rangle$  [nm],  $\text{H}_2\text{O}$ ):  $23 \pm 2$ . G4 (UV-vis,  $\lambda_{\text{max}}$  [nm],  $\text{H}_2\text{O}$ ): 525; DLS ( $\langle 2\text{RH} \rangle$  [nm],  $\text{H}_2\text{O}$ ):  $27 \pm 2$ . G5 (UV-vis,  $\lambda_{\text{max}}$  [nm],  $\text{H}_2\text{O}$ ): 530; DLS ( $\langle 2\text{RH} \rangle$  [nm],  $\text{H}_2\text{O}$ ):  $35 \pm 2$ ; (Z-pot [mV],  $\text{H}_2\text{O}$ ): -39

The synthesis of Au-PEG-NH<sub>2</sub> nanoparticles requires the preliminary preparation of PEG polymer, hereafter reported according to Howarth and collaborators [21].

**2.2.2.1 PEG polymer synthesis:** According to a precedent protocol developed by Schladt [22] and Howarth [21], to a solution of lipoic acid (LA) (5 g, 24.23 mmol) and *N*-Hydroxysuccinimide (NHS) (3.35 g, 29.1 mmol) in 150 mL THF at 0 °C was added slowly to a solution of dicyclohexylcarbodiimide (DCC) (6.00 g, 29.1 mmol) in 10 mL THF. The mixture was warmed to room temperature and stirred for 5 h. The precipitate was removed by vacuum filtration and the solvent evaporated *in vacuo*. The crude product was re-dissolved in 100 mL of ethyl acetate and filtered once more by vacuum filtration. The product was re-crystallized from a solution of hot ethyl acetate:hexane (1:1 v/v) as a pale yellow solid (5.88 g, 80%). Yield is 80%. The product is confirmed by NMR and ESI-MS. <sup>1</sup>H NMR (400 MHz,  $\text{CDCl}_3$ )  $\delta$  3.66-3.61 (m, 1H), 3.26-3.15(m, 2H) 2.85(s, 4H), 2.69-2.67(t, 2H), 2.55-2.49(m, 1H), 2.01-1.95(m, 1H), 1.86-1.74(m, 5H), 1.64-1.57(m, 2H). ESI-MS: Calculated for  $\text{C}_{12}\text{H}_{17}\text{NO}_4\text{S}_2\text{Na}$ : 326.04 Found : 326.09 NMR and rough ESI-MS Spectrum are reported respectively in Figure 2S and Figure 3S in the Supporting Materials.

To a stirred solution of the PEG1500-bisamine (1000mg 0.64 mmol) and triethylamine (90  $\mu\text{l}$ , 0.64 mmol) in 20 mL of 1,4-dioxane was added dropwise a solution of lipoate-NHS ester (150 mg, 0.8 eq. 0.51 mmol) in 4 ml of 1,4 dioxane over 2 h. The reaction mixture was allowed to stand overnight until thin layer chromatography (TLC) analysis showed no lipoate-NHS ester remaining. After the solvent was evaporated, the crude product LA-PEG-NH<sub>2</sub> was purified by alumina column (dichloromethane /methanol 95:5). Yield is 70%. ESI-MS:  $m/z$  1689  $[\text{M} + \text{H}]^+$

**2.2.2.2 Ligand Exchange:** To a stirring 4 ml solution of Gold nanocores (0.5 nM) we gently added 0.4 ml ethanol/water (1:1) of LA-PEG-NH<sub>2</sub> (5mM). The solution was kept on stirring overnight. The obtained Au-PEG-NH<sub>2</sub> nanoparticles were then purified from the solution by means of Amicon Ultra-15 centrifugal filtration for 5 min at 1900 g twice. Main characterizations of the product are herein reported. Au-PEG-NH<sub>2</sub> (UV-vis,  $\lambda_{\max}$  [nm], H<sub>2</sub>O): 532; DLS (<2RH> [nm], H<sub>2</sub>O):  $40 \pm 2$  (Z-pot [mV], H<sub>2</sub>O): +29. IR-Spectrum is reported in Figure 4S in the Supporting Materials.

### 2.3 “In situ” coupling of glucuronic acid to Au-PEG-NH<sub>2</sub> nanoparticles

To a solution of 0.5 ml (2 nM) of Au-PEG-NH<sub>2</sub> a 0.5 ml water solution of glucuronic acid (1.94 mg, 10  $\mu$ mol) was added. After that, the compound N-(3-Dimethylaminopropyl)-N'-ethylcarbodiimide EDC (5.82 mg, 30  $\mu$ mol) in powder was added to the stirring solution and kept in stirring for 1 hour. Subsequently, 100 microliter of NaHCO<sub>3</sub> 0.1 M was added to the mixture. The activated glucuronic acid solution was then transferred in a vial containing the Au-PEG-NH<sub>2</sub> nanoparticles solution (0.5 ml of 2 nM) and kept in stirring for 3 hours. The Au-PEG-Glu nanoparticles were purified by means of Amicon Ultra-15 centrifugal filtration (5 min at 1900 g twice) of the final solution, giving the solid Au-PEG-Glu nanoparticles. Main characterizations of the product are herein reported.

Au-PEG-Glu (UV-vis,  $\lambda_{\max}$  [nm], H<sub>2</sub>O): 532; DLS (<2RH> [nm], H<sub>2</sub>O):  $40.5 \pm 2$  (Z-pot [mV], H<sub>2</sub>O): +30. IR-Spectrum is reported in Figure 4S in the Supporting Materials.

### 2.4. Characterization Methods

UV-Vis Absorption spectra of gold nanoparticles dispersed in deionized water were measured in 1.00 cm optical path quartz cells by using a Cary 100 Varian spectrophotometer. Dynamic light scattering (DLS) measurements were carried out on the nanoparticle aqueous suspensions (1.0–0.20 mg/mL), using a Brookhaven instrument (Brookhaven, NY) equipped with a 10 mW HeNe laser at a 632.8 nm wavelength at a temperature of  $(25.0 \pm 0.2)^\circ\text{C}$ . Z-Potential was measured using the laser Doppler velocimetry technique (Malvern Nano ZS90 instrument) and particle velocity was expressed per unit field strength as the electrophoretic mobility  $u$ . The Z-Potential was calculated using the Henry equation [23].

Fourier Transform – Infra Red (FT-IR) measurements were performed in Attenuated Total Reflectance (ATR) mode by means of The FT/IR-4700 instrument in the spectral range from  $500\text{ cm}^{-1}$  to  $4000\text{ cm}^{-1}$ .

Extractive Electrospray Ionization - Mass Spectrometry (ESI-MS) measurements were performed for characterization of PEG polymers. The ESI-MS was performed by means of Liquid Chromatography – coupled to Time Of Flight detector (LC-TOF) and Matrix-Assisted Laser Desorption Ionization - coupled to Time Of Flight detector (MALDI-TOF). ESI-MS was performed using a Waters LCT Premier system. For all ESI-MS measurements, product was dissolved in methanol.

Nuclear Magnetic Resonance (NMR) spectroscopy was carried out by means of Bruker Avance spectrometers (400 MHz) using CDCl<sub>3</sub> as solvent.

## 2.4. Biological Methods

**Cell lines and culture conditions**—HeLa cells were cultured in EMEM (EuroClone, Pero, Italy) medium supplemented with 10% foetal bovine serum (FBS) (EuroClone, Pero, Italy), 100 units/mL penicillin and 100 mg/mL streptomycin, and 2 mM L-glutamine, and grown in 5% CO<sub>2</sub> atmosphere at 37°C. In these conditions, the cell doubling time was 24 ± 1 hour.

**Glut-1-GFP Transfection condition**—Glut-1-GFP plasmid was purchased by ADDGenes plasmid bank. Transfections were by a liposome-mediated method. One day before transfection, cells were plated on a coverslip in 35mm dishes at 40-50% confluence. After one day's growth, transfections were performed using 1.5 µg of each relevant plasmid and LIPOFECTAMINE 2000™ transfection reagent (Invitrogen) according to the manufacturer's instructions.

## 2.5 Biophysical Methods

**2.5.1 Orbital tracking**—All the tracking experiments were carried out with an Olympus IX70 microscope (Fig. 1). The two-photon excitation source was a mode-locked titanium-sapphire laser (Mira 900; Coherent; Palo Alto, CA) pumped by an argon ion laser (Innova 300; Coherent) and tuned at 780 nm. The laser power at the sample ranged from 1 to 10 mW. The light is directed into the microscope by two galvomotor-driven scanning mirrors (Cambridge Technologies, Watertown, MA) through a scanning lens. The laser light is reflected with a low-pass dichroic mirror (transmission from 370 nm to 630 nm; Chroma Technology; Brattleboro, VT) and focused on the sample with a 20× (dry) 0.75-NA plan apochromat objective. Fluorescence emission was collected by the objective and passed through a dichroic and short-pass filter to eliminate any reflected excitation light. It then exits the microscope to the detector (Hamamatsu (Tokyo, Japan) H7422P-40 photomultiplier tube) on the side port. The output of this unit was amplified and passed through a discriminator (PX01 Photon Counting Electronics; ISS; Champaign, IL). Photons were counted with a data acquisition card (ISS). During the tracking procedure, the two scanning mirrors are moved independently by voltages generated in a computer card (3-axis card; ISS). When they are synchronized to move following sine waves shifted 90° relative to one another, the laser beam moves in a circular path. The position of the scanning center is determined by the offset values of the sine waves. A piezoelectric z-nanopositioner (Polytec PI; Auburn, MA) equipped with a linear voltage differential transformer feedback sensor and operated in closed-loop configuration is placed below the objective to enable changes of the focal plane. During each cycle of the tracking routine, the 3-axis card generates a square wave voltage that drives the motion of the z-nanopositioner between two z planes separated by a distance given by the amplitude of the square wave. Similar to the x and y coordinates, the position of the center of z-scanning is given by the DC offset. The experiments are controlled by a data acquisition program (SimFCS; LFD; Champaign, IL). This program, which also contains the tools used for trajectory analysis, can be downloaded from the Laboratory for Fluorescence Dynamics website ([www.lfd.uiuc.edu](http://www.lfd.uiuc.edu)).

In order to perform Infrared Differential interference contrast (IR-DIC) imaging, the microscope was modified with an IR LED (Optodiode, Newbury Park, CA) and a cMOS camera (Pixelink; Ottawa, ON, Canada) according to Levi and collaborators [24].

**2.5.2 Pair Correlation Analysis (pCF)**—Calculation of the pair-correlation functions was done using the SIMFCS software developed at the Laboratory for Fluorescence Dynamics ([www.lfd.uci.edu](http://www.lfd.uci.edu)), as described in previously published articles [6]. Intensity data are presented by using a carpet representation in which the x coordinate corresponds to the point along the line (pixels) and the y coordinate corresponds to the time of acquisition. The pair correlation functions (pCF, pixels) are displayed in pseudo-color in an image in which the x coordinate corresponds to the point along the line and the y coordinate corresponds to the pair correlation time in a log scale. The distance at which pCF analysis were carried out were fixed at 8 pixels (which corresponds to 256 nm) across all experiments.

### 3. Results and Discussions

#### 3.1. Synthesis and characterization of stabilized gold nanoparticles

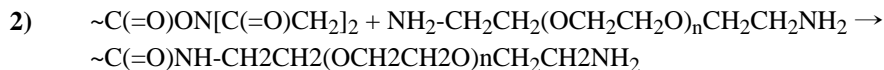
The present study is mainly focused on glucose capped gold nanoparticles uptake in living cells. For this purpose, the development of a proper model of GNPs was mandatory in order to investigate the GNPs fate during the uptake process. Currently, GNPs synthesis is a growing research theme [2, 25, 26]. A recent work reports on the synthesis of GNPs capped with 3mercaptopropylsulfonate and 1-thiogluconate, which show enhanced cell internalization, short term cytotoxicity and long term cell killing, when tested “in vitro” for HSG cells [16]. However, our work further improves the existing GNPs functionalization procedures by means of a new development: the exploiting of the facile NHS chemistry [20] together with use of PEG as surface stabilizer agent [21, 27]. The overall synthetic procedures include the gold-core synthesis, the polymer synthesis and further derivatization steps, which are described in material and methods section and fully reported in Schemes 1, 2, 3. The gold-nanocores were synthesized using a well-known literature method [19], which consists in wet reduction of tetrachloroauric acid to metallic gold by means of sodium citrate as reducing agent. Preliminary studies performed on these nanoparticles showed their hydrodynamic DLS size in the range 35-40 nm, while the UV–Vis spectrum, showed the typical Surface Plasmon Resonance band in the 520-540 nm range confirming the nanosize of the gold core (Supporting Materials: Figure 1S). As previously stated, the proposed synthetic route relies on the NHS chemistry in order to obtain the glucose derivatization of GNPs surface. NHS is a coupling agent molecule, which can induce the formation of very reactive esters on the carboxylic acid moieties. Thereafter, activated esters can react with amines to form stable amides bonds. Regarding the stabilizing agent of GNPs surface, our choice was oriented to the use of PEG as starting polymer, considering its efficiency in the stabilization and the hydrophilic character of the already studied Au-PEG-NH<sub>2</sub> [21,27]. Hence, exploiting the NHS coupling reaction, a both thiol and primary amine ends of PEG polymer was obtained in two steps, as shown in Scheme 1. In particular, during the first step reaction the formation of LA-NHS amide takes place according to:





NHS ester of lipoic acid formation was proven by NMR spectrum reported in supporting materials (Supporting Materials: Figure 2S and ) and ESI-MS (Supporting Materials: Figure 3S).

The second step finally leads to LA-PEG-NH<sub>2</sub> polymer formation as reported in reaction scheme below:



The formation of expected amide bonds was assessed by means of FT-IR spectroscopy. The IR-spectra of the LA-PEG-NH<sub>2</sub> polymer are reported in Supporting Materials Figure 4S and showed the typical amide stretching signal in the range 1670-1690 cm<sup>-1</sup>. The results of ESI-MS analysis reported in Figure 1 revealed the occurrence of two peaks in the range 600-800 Da, assignable to the polymer fragmentation. However, due to the crosslinking between two monomers chains, also other peaks representing twice the expected weight of the polymer are present. Rough ESI-MS spectra are reported for both NH<sub>2</sub>-PEG-NH<sub>2</sub> and LA-PEG-NH<sub>2</sub> in Figure 5S of Supporting Materials.

Exploiting the strong affinity between sulphur and gold atoms, a ligand exchange reaction was performed, as shown in Scheme 2, in order to bind the synthetic polymer on the GNPs surface. The fulfilment of the reaction was proven by means of DLS and Z-Potential measurements. The GNPs after the ligand exchange reactions, named Au-PEG-NH<sub>2</sub>, showed an increased Hydrodynamic Radius compatible with the theoretical polymer length of 3 nm, also reported in Figure 2.

The overall surface NPs charge, from the negative value of -39 mV for the citrate capped gold cores, turned out to a positive value of +29 mV due the primary amine protonation. The Z-Potential inversion is a crucial point to assess the polymer binding as already described elsewhere [28]. Besides this, the overall surface charge plays a fundamental role in the stability of particles in the media. The charge, positive (more than +25 mV) or negative (less than -25 mV) prevents aggregation due to electrostatic repulsive force [29]. The nature of chemical interaction between the sulfur and the gold atom (~45 kcal/mol) [19] is responsible for further stability of the system. The binding geometry, the structural arrangement of the thiols and the PEG folding on NPs surface are currently appealing topics [30]. However, due the complexity and challenging nature of the investigation a deep chemical and spectroscopic characterization of PEG-Gold surface interaction will be the aim of future study. The DLS and Z-Potential results for all particles at the different synthetic stages are summed up in Table 1.

As reported in Scheme 3, the final synthetic step involved the GNP-Glucose functionalization *in situ* throughout the already reported NHS chemical strategy. The glucuronic acid (GA) molecule was selected as reagent due the presence of carboxylic function essential for the NHS esterification. Moreover, despite the carboxyl group, GA still possesses the appropriate chemical structure to properly bind to GLUT-Receptor [31].

After the final step reaction, the resulting GNPs named Au-PEG-Glu showed no significant changes in the DLS and Z-Potentials measurements. Despite that, Au-PEG-Glu

nanoparticles seem to possess the glucose functionalities anyway. Indeed, a qualitatively analysis of confocal pictures cells treated with GNPs suggest a selective binding to cell membrane glucose marked receptor. For the sake of clarity, an example of specific binding picture is reported in Figure 3. The picture shows HeLa cells treated with Au-PEG-Glu (A-B-C) or Au-PEG-NH<sub>2</sub> (D-E-F). Images were acquired in three channels: Fluorescence (A-D), Scattering (B-E), Transmission (C-F). Fluorescence mode allows to localize the GFP-fused Glut-1 receptor while the scattering channel highlights the GNPs position. The comparison of transmission and fluorescence channels clearly illustrates a specific Au-PEG-Glu binding to the cell membrane glucose receptor.

### 3.3. Biophysical experiments: nanoparticles uptake mechanism

**3.3.1. Orbital Tracking**—Particle tracking is an appealing approach to study uptake process because it can provide a detailed description of the initial interaction between the cell and the particle as well as the characteristics of the motion and the destination of the particle in the cell [24, 32]. We exploit the power of the 3-D particle tracking method in order to characterize the uptake of gold glucose nanoparticles by HeLa Cells. According to similar work [24], the synthesized GNPs were incubated in the culture medium with HeLa cells previously starved in Dulbecco's phosphate buffered saline for 2 h at 37°C. To select the nanoparticle that are interacting with the cells, we registered simultaneously the Infrared Differential interference contrast (IR-DIC) and fluorescence images of the sample. The fluorescence image allows us to detect a fluorescent receptor expressed on cell membrane, whereas the IR-DIC image provides the details of its position with respect to the cell and allows us to follow the motion of the cell during the tracking. Figure 4 shows a two-dimensional (2-D) projection of trajectories for Nanoparticles bound to the receptor moving according to this description overlapped with the DIC images of the cells.

**3.3.2. pCF**—The pCF method is based on the spatiotemporal correlation of the position of the same particle at a given distance and a given time. As well described by Gratton and collaborators [17], pCF algorithm can recognize and separate families of molecules that diffuse at different rates. Consequently, obstacles to diffusion can be detected, as in our case the NP-GLUT1 complex crossing throughout the cell membrane.

Figure 5 shows the results of the pCF experiment. The frequencies reported indicate the events with the relative Diffusion coefficient. Figure 6 (a-b) shows the carpet and the pCF analysis for Au-PEG-Glu during the uptake. The pCF(8) shows a discontinuity in the correlation at a given position along the orbit. The autocorrelation at each column gives the average diffusion coefficient and is reported in figure 6-a. The NP-GLUT1 complex has a diffusion coefficient of 0.129  $\mu\text{m}^2/\text{s}$ . In figure 6-b, the detail of the pCF at column 150 along the line scan shows the complex delay in reaching a distance of 8 pixels (256 nm).

From the comparison of related work in the literature, the diffusion coefficient value found for our complex suggests the involvement of endocytotic pathway [33].

## 4. Summary & Conclusions

A new kind of biocompatible and very stable nanoparticles, Au-PEG-Glu, has been synthesized with the purpose of increasing the amount of gold atoms inside the cell. The synthesis was optimized to obtain nanoparticles diameter in a range that maximizes the uptake in cells. Nanoparticles physical values *i.e.* HydroDynamic Radius and Z-Potential show that glucose molecules are still present on the NPs surface as demonstrated qualitatively by means of confocal microscopy. Moreover, a detailed investigation about the biophysical proprieties of Au-PEG-Glu complex by means of FCS techniques was carried out. The study gives new insights about the uptake mechanism of Gold nanoparticles capped with glucose molecules.

The data analysis showed that the diffusion coefficient of the Gold NPs inside the cells is  $0.129 \mu\text{m}^2/\text{s}$ , suggesting an uptake mechanism driven by endocytosis pathway. The complex Au-PEG-Glu was tracked inside the cells and its trajectory and diffusions coefficient was also recorded.

In conclusion, by means of the present work a new approach for the synthesis of a new kind of stable and positively charged and Glucose functionalized nanoparticles was developed. The Glucose capped GNPs are suitable for improved radiotherapy and drug delivery applications. Moreover, a characterization regarding the receptor complex fate was also performed. However, further chemical characterization on the glucose bonding appears mandatory for future studies.

## Supplementary Material

Refer to Web version on PubMed Central for supplementary material.

## Acknowledgments

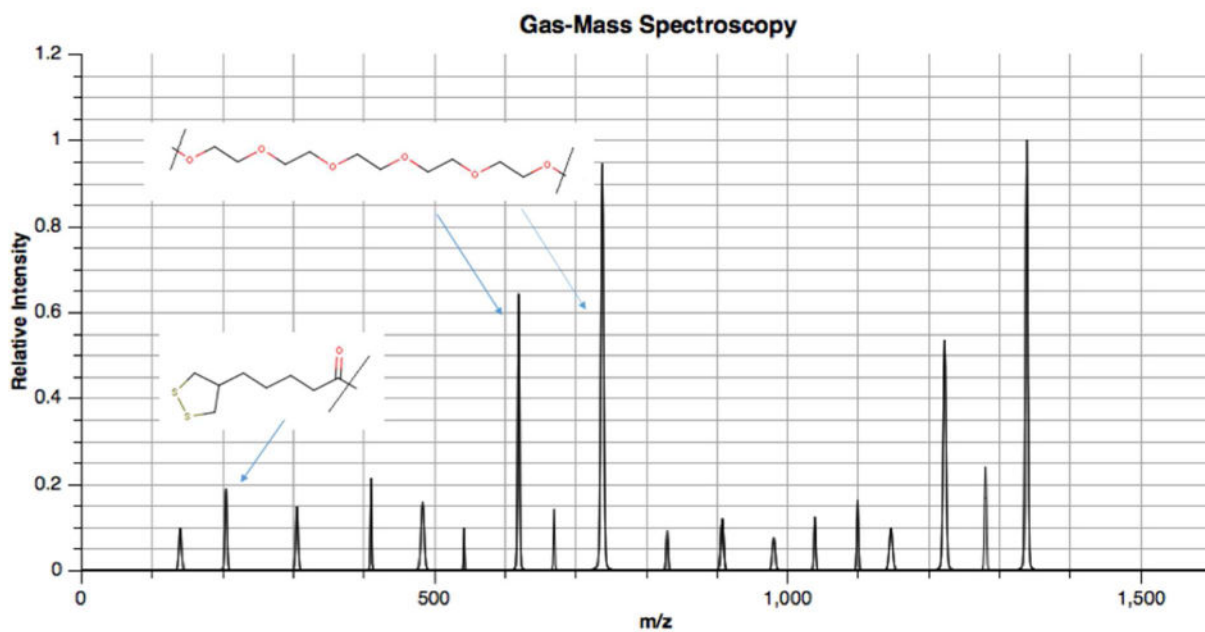
Dr. Francesco Porcaro gratefully acknowledge the Ph.D. programme “Scienze e Tecnologie Biomediche” of the Department of Sciences, Roma Tre University; The experiments reported in this paper were performed at the Laboratory for Fluorescence Dynamics (LFD) at the University of California, Irvine (UCI). The LFD is supported jointly by the National Institutes of Health (8P41GM103540) and UCI

## References

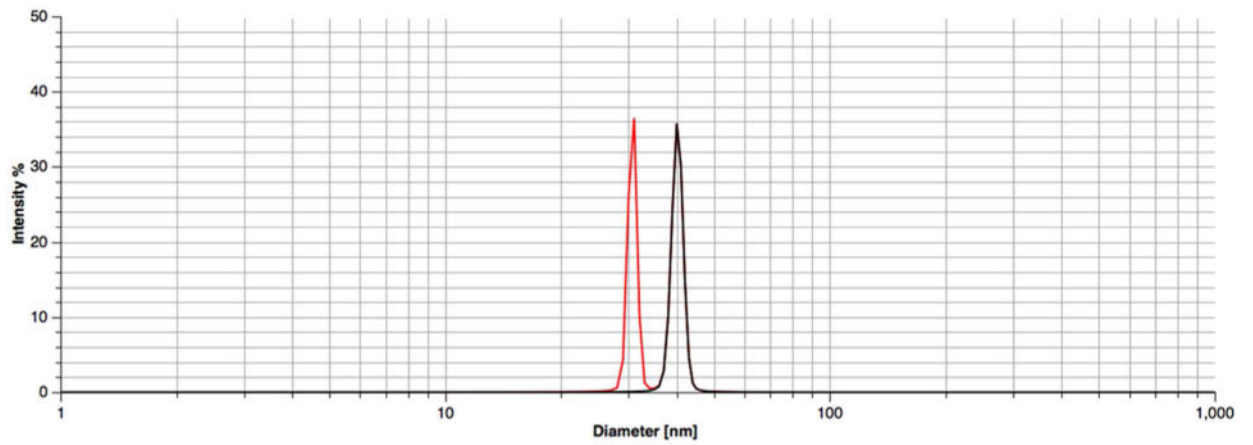
1. Zeng C, Jin R. Gold nanoclusters: Size-controlled Synthesis and Crystal Structures. *Struct Bond*. 2014; 161:87–115.
2. Fratoddi I, Venditti I, Cametti C, Russo MV. Gold Nanoparticles and Gold Nanoparticle-conjugates as Drug Delivery Vehicles. *Progress and Challenge. J Mater Chem B*. 2014; 2:4204–4220.
3. Cole LE, Ross RD, Tilley JM, Vargo-Gogola T, Roeder RK. Gold Nanoparticles as Contrast Agents in X-ray Imaging and Computed Tomography. *Nanomedicine*. 2015; 10:321–341. [PubMed: 25600973]
4. Ghosh P, Han G, De M, Kim CK, Rotello VM. Gold Nanoparticles in Delivery Applications. *Adv Drug Deliver Rev*. 2008; 60:1307–1315.
5. Dreaden EC, Alkilany AM, Huang X, Murphy CJ, ElSayed MA. The Golden Age: Gold nanoparticles for Biomedicine. *Chem Soc Rev*. 2012; 41:2740–2779. [PubMed: 22109657]

6. Cametti C, Fratoddi I, Venditti I, Russo MV. Dielectric Relaxations of Ionic Thiol-Coated Noble Metal Nanoparticles in Aqueous Solutions: Electrical Characterization of the Interface. *Langmuir*. 2011; 27:7084–7090. [PubMed: 21563807]
7. Venditti I, Palocci C, Chronopoulou L, Fratoddi I, Fontana L, Diociaiuti M, Russo MV. Candida rugosa Lipase Immobilization on Hydrophilic Charged Gold Nanoparticles as Promising Biocatalysts: Activity and Stability Investigations. *Colloids Surfaces B*. 2015; 131:93–101.
8. Austin LA, Mackey MA, Dreaden EC, El-Sayed MA. The Optical, Photothermal, and Facile Surface Chemical Properties of Gold and Silver Nanoparticles in Biodiagnostics, Therapy, and Drug Delivery. *Arch Toxicol*. 2014; 88:1391–1417. [PubMed: 24894431]
9. Fratoddi I, Venditti I, Cametti C, Russo MV. How Toxic Are Gold Nanoparticles? The State-of-the-Art Nano Research. 2015; 8:1771–1799.
10. Kong T, Zeng J, Wang X, Yang X, Yang J, McQuarrie S, McEwan A, Roa W, Chen J, Xing JZ. Enhancement of Radiation Cytotoxicity in Breast-Cancer Cells by Localized Attachment of Gold Nanoparticles. *Small*. 2008; 4:1537–1543. [PubMed: 18712753]
11. Zhang X, Xing JZ, Chen J, Ko L, Amanie J, Gulavita S, Pervez N, Yee D, Moore R, Roa W. Enhanced Radiation Sensitivity in Prostate Cancer by Gold-Nanoparticles. *Clin Invest Med*. 2008; 31:160–167.
12. Roa W, Zhang X, Guo L, Shaw A, Hu X, Xiong Y, Gulavita S, Patel S, Sun X, Chen J, Moore R, Xing JZ. Gold Nanoparticle Sensitize Radiotherapy of Prostate Cancer Cells by Regulation of the Cell Cycle. *Nanotechnology*. 2009; 20:375–101.
13. Roa W, Xiong Y, Chen J, Yang X, Song K, Yang X, Kong B, Wilson J, Xing JZ. Pharmacokinetic and Toxicological Evaluation of Multi-functional Thiol-6-fluoro-6-deoxy-D-glucose Gold Nanoparticles in Vivo. *Nanotechnology*. 2012; 23:375101. [PubMed: 22922305]
14. Gromnicova R, Davies HA, Sreekanthreddy P, Romero IA, Lund T, Roitt IM, Phillips JB, Male DK. Glucose-coated Gold Nanoparticles Transfer Across Human Brain Endothelium and Enter Astrocytes in Vitro. *PLoS One*. 2013; 8:81043.
15. Cai W, Gao T, Hong H, Sun J. Applications of Gold Nanoparticles in Cancer Nanotechnology. *Nanotechnol Sci Appl*. 2008;1. [PubMed: 24198457]
16. Porcaro F, Battocchio C, Antocchia A, Fratoddi I, Venditti I, Fracassi A, Luisetto I, Russo MV, Polzonetti G. Synthesis of Functionalized Gold Nanoparticles Capped with 3-Mercapto-1-propansulfonate and 1-Thioglucose Mixed Thiols and “in Vitro” Bioresponse. *Colloids Surfaces B*. 2016; 142:408–416.
17. Digman MA, Gratton E. Imaging Barriers to Diffusion by Pair Correlation Functions. *Biophysical Journal*. 2009; 97:665–673. [PubMed: 19619481]
18. Lanzanò L, Gratton E. Orbital Single Particle Tracking on a Commercial Confocal Microscope Using Piezoelectric Stage Feedback. *Methods Appl Fluoresc*. 2014;2.
19. Bastus NG, Comenge J, Puentes V. Kinetically Controlled Seeded Growth Synthesis of Citrate-Stabilized Gold Nanoparticles of up to 200 nm: Size Focusing versus Ostwald Ripening. *Langmuir*. 2011; 27:11098–11105. [PubMed: 21728302]
20. Hermanson, GT. *Bioconjugate Techniques*. 3. Academic Press; London, U.K.: 2013.
21. Howarth M, Liu W, Puthenveetil S, Zheng Y, Marshall LF, Schmidt MM, Wittrup KD, Bawendi MG, Ting AY. Monovalent, Reduced-size Quantum Dots for Imaging Receptors on Living Cells. *Nat Methods*. 2008; 5:397–399. [PubMed: 18425138]
22. Schladt TD, Schneider K, Shukoor MI, Natalio F, Bauer H, Tahir MN, Weber S, Schreiber LM, Schröder HC, Müller WEG, Tremel W. Highly Soluble Multifunctional MnO Nanoparticles for Simultaneous Optical and MRI Imaging and Cancer Treatment Using Photodynamic Therapy. *J Mater Chem*. 2010; 20:8297–8304.
23. Somasundaran, P. *Encyclopedia of Surface and Colloid Science Second Edition*. CRC Press; Boca Raton, U.S.A: 2006.
24. Levi V, Ruan Q, Gratton E. 3-D Particle Tracking in a Two-Photon Microscope: Application to the Study of Molecular Dynamics in cells. *Biophys J*. 2005; 88:2919–2928. [PubMed: 15653748]
25. Katti KK, Kattumuri V, Bhaskaran S, Katti KV, Kannan R. Facile and General Method for Synthesis of Sugar-Coated Gold Nanoparticles. *Int J Green Nanotechnol Biomed*. 2009; 1:B53–B59. [PubMed: 20011668]

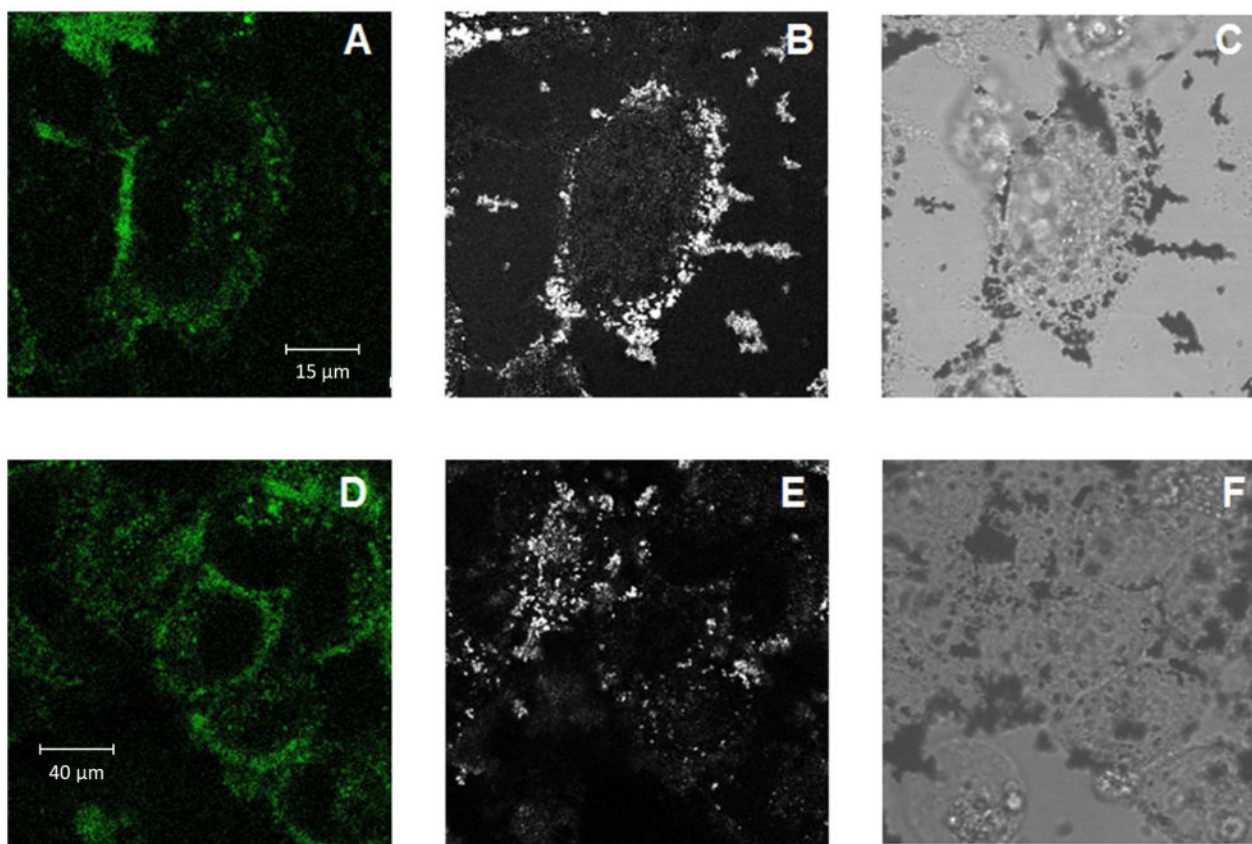
26. Salehizadeh H, Hekmatian E, Sadeghi M, Kennedy K. Synthesis and Characterization of core-shell Fe<sub>3</sub>O<sub>4</sub>-Gold-chitosan Nanostructure. *J Nanobiotechnology*. 2012;10. [PubMed: 22409971]
27. Rahme K, Chen L, Hobbs RG, Morris MA, O'Driscolle C, Holmesab JD. PEGylated Gold Nanoparticles: Polymer Quantification as a Function of PEG Lengths and Nanoparticle Dimension. *RSC Adv*. 2013; 3:6085–6094.
28. Kawano T, Niidome Y, Katayama Y, Niidome T. PEG-Modified Cationic Gold Nanoparticles and Their Abilities of In Vivo Gene Delivery. *Molecular Therapy*. 2005; 11:S84.
29. Hanaor DAH, Michelazzi M, Leonelli C, Sorrell CC. The Effects of Carboxylic Acids on the Aqueous Dispersion and Electrophoretic Deposition of ZrO<sub>2</sub>. *J Eur Ceram Soc*. 2012; 32:235–244.
30. Häkkinen H. The Gold–Sulfur Interface at the Nanoscale. *Nature Chemistry*. 2012; 4:443–455.
31. Calvaresia EC, Hergenrothera PJ. Glucose Conjugation for the Specific Targeting and Treatment of Cancer. *Chem Sci*. 2013; 4:2319–2333. [PubMed: 24077675]
32. Anzalone A, Annibale P, Gratton E. 3D Orbital Tracking in a Modified Two-photon Microscope: An Application to the Tracking of Intracellular Vesicles. *J Vis Exp*. 2014; 92:51794.
33. Chithrani DB. Use of Gold Nanoparticles as a Model System to Optimize Interface Between Medicine and Nanotechnology. *Insciences J*. 2011; 1:115–135.



**Figure 1.** ESI-MS spectrum of the LA-PEG-NH<sub>2</sub> polymer shows two peaks in the range 600-800 Da, assignable to the polymer fragmentation.

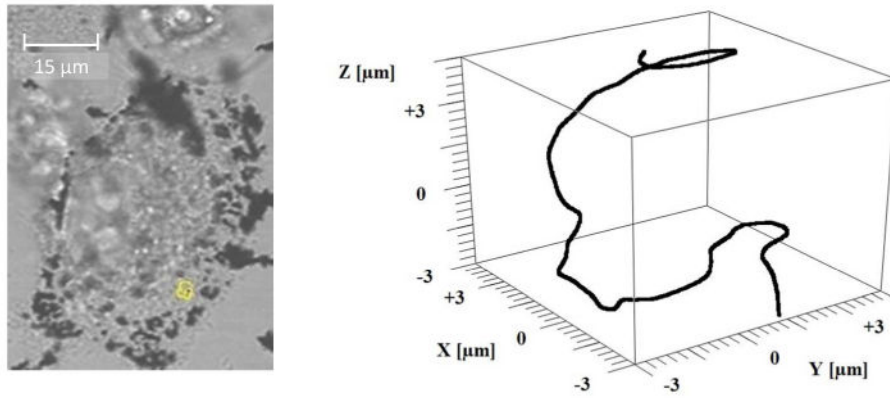


**Figure 2.** DLS spectra of gold cores stabilized with citrate anions (in red) and Au-PEG-NH<sub>2</sub> (in black). The PEG polymer increased Hydrodynamic Diameter of the particles.

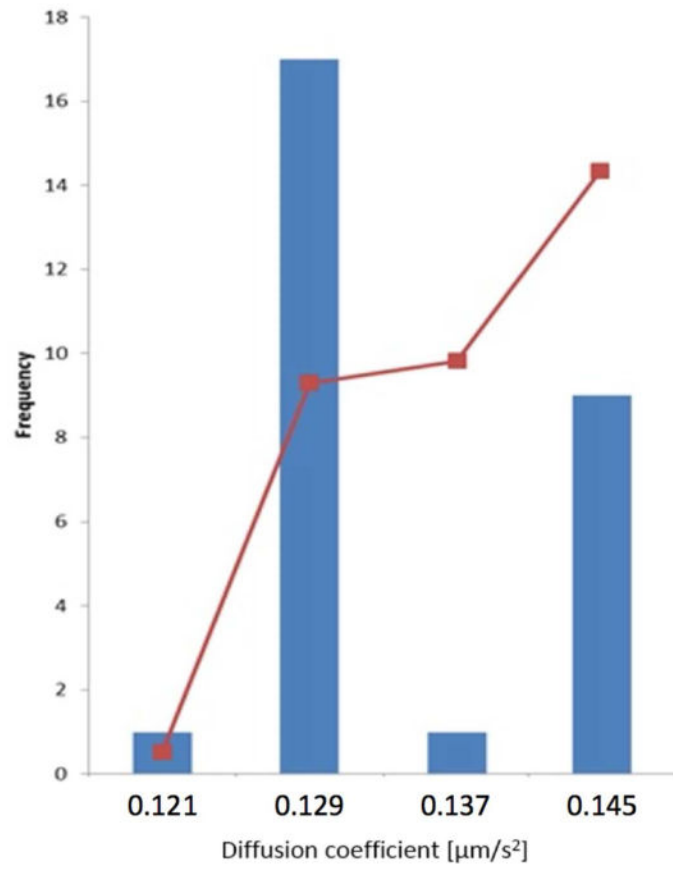


**Figure 3.** Raw data images of HeLa cells treated with Au-PEG-Glu (A-B-C) or Au-PEG-NH<sub>2</sub> (D-E-F). Images are acquired in three channel: Fluorescence (A-D), Scattering (BE), Transmission (C-F). The scattering images comparison (B-E) shows clearly the Au-PEG-Glu bind specific to cell membranes.

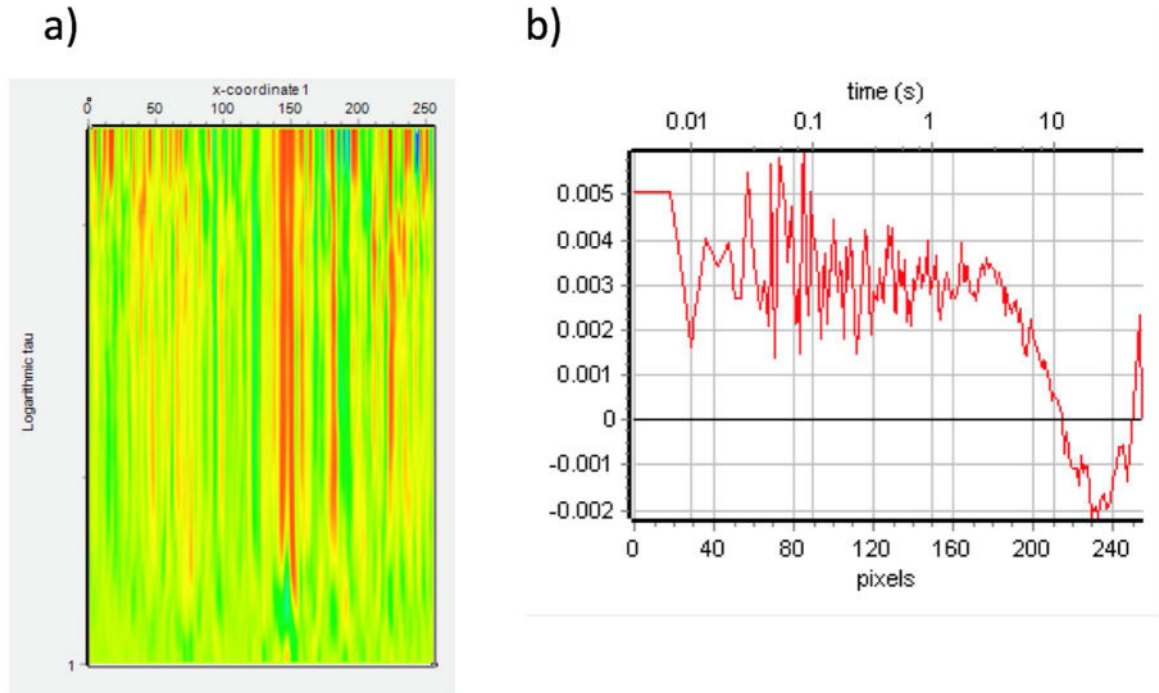




**Figure 4.** Uptake of Au-PEG-Glu and Trajectories of a complex NP-receptor. The yellow lines correspond to the 2-D projections of the trajectories.

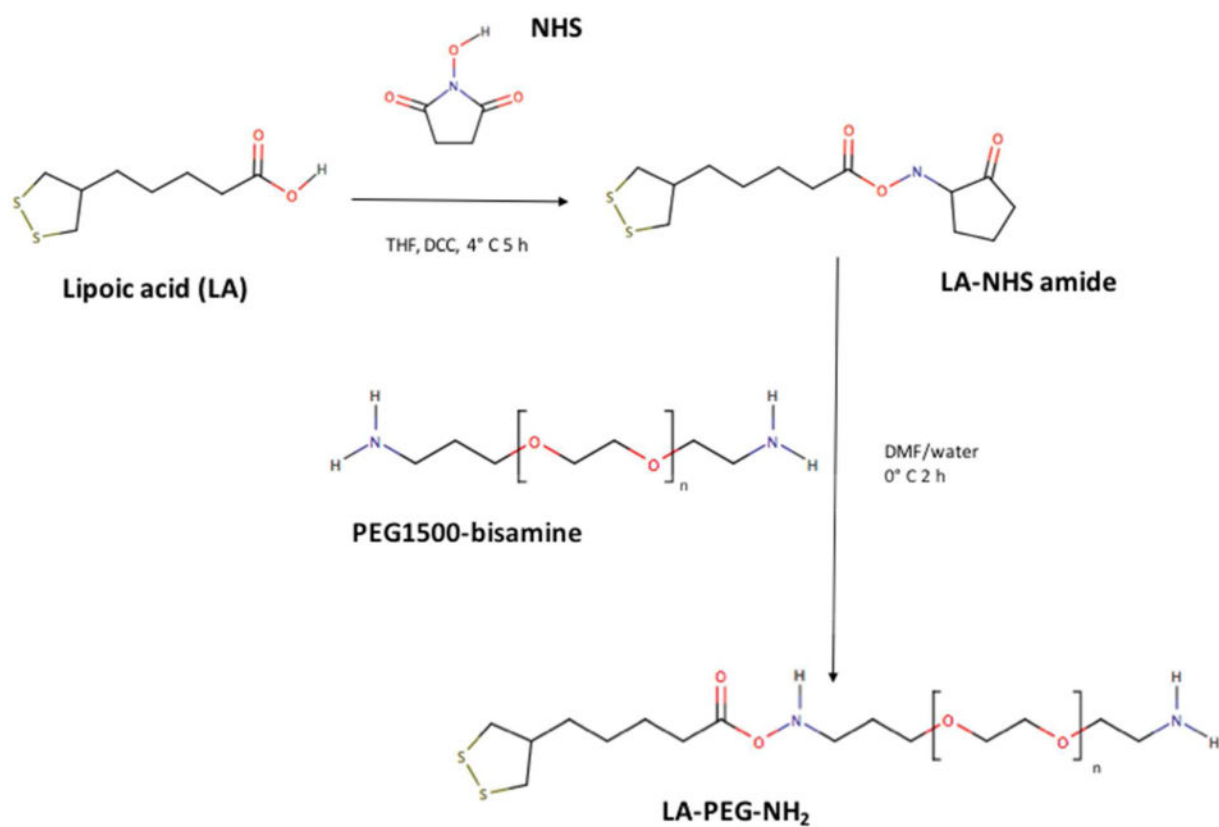


**Figure 5.**  
Frequency events for uptake GNP bound to Glut-transporter

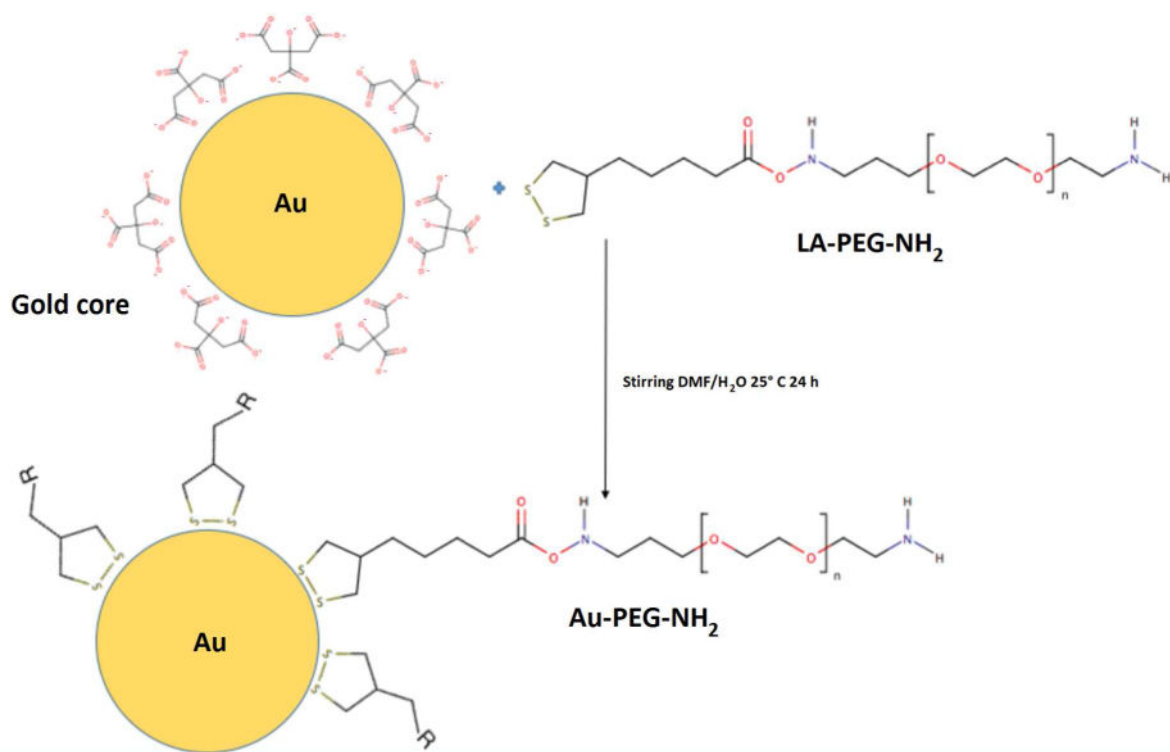


**Figure 6.**

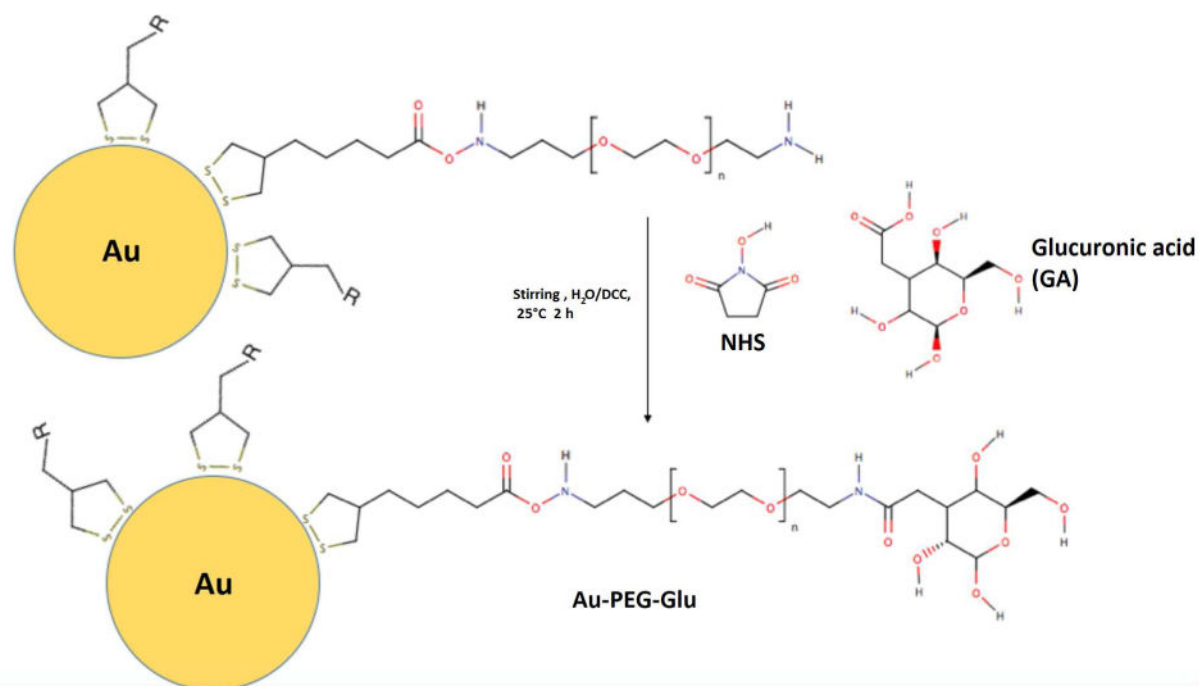
The autocorrelation at each column gives the average diffusion coefficient. The NP-GLUT1 complex has a diffusion coefficient of  $0.129 \mu\text{m}^2/\text{s}$  a) pCF(8) Carpet b) Tau graph;



**Scheme 1.**  
Synthetic procedure for the synthesis of LA-PEG-NH<sub>2</sub> polymer.

**Scheme 2.**

General reaction scheme for ligand exchange reaction leading to Au-PEG-NH<sub>2</sub> nanoparticles

**Scheme 3.**

Synthetic procedure for *in situ* glucuronic acid conjugation to obtain Au-PEG-Glu nanoparticles.

**Table 1**

Characterizations on Au-NP (solvent water). Second column shows the value of UV-visible Plasmon while respectively third and fourth columns DLS and Z-Potential measurements.

Sample Name	UV-Vis Plasmon [nm]	HydroDynamic Diameter by DLS [nm]	Z- Potential value [mV]
Gold core	530	34±2	-39±1
Au-PEG-NH <sub>2</sub>	532	40±2	+29±1
Au-PEG-GLU	532	40±2	+30±1

Author Manuscript

Author Manuscript

Author Manuscript

Author Manuscript